JOURNAL OF PROPULSION AND POWER
Vol. 22, No. 2, March–April 2006

Transient Burning Characteristics of JA2 Propellant Using Experimentally Determined Zel'dovich Map

Kenneth K. Kuo* and Baoqi Zhang†
Pennsylvania State University, University Park, Pennsylvania 16802

Combustion characteristics of JA2 propellant were studied both experimentally and theoretically. Its steady-state burning behavior was investigated using an optical strand burner. The parameters measured were the regression rate, subsurface temperature profile, and burning surface temperature at different initial temperatures ($-40 < T_i < 80$°C) and pressures ($0.1 < P < 68$ MPa). The measured burning rates r_b were correlated as a function of T_i and pressure up to 300 MPa. Predicted r_b from the correlation are in close agreement with experimental data. The temperature sensitivity σ_p was found to decrease as pressure increases, reaching an asymptotic value of 0.0024 K^{-1} at high pressures. Surface-temperature data were correlated as a linear function of pressure with temperature-dependent coefficients. The Zel'dovich map was constructed from the experimental data. This map was then used in a computer simulation to investigate the transient burning characteristics of JA2 under different pressurization rates. From the simulation results, it was found that JA2 propellant only exhibits a mild transient burning effect. This finding is further confirmed with the observations obtained from a parallel experimental study using an interrupted burner coupled with a real-time X-ray radiography. The reason for this finding is the low value of σ_p and its rapid decay as the pressure increases for $P < 20$ MPa.

Nomenclature

A	=	preexponential coefficient of the Arrhenius pyrolysis law
a	=	preexponential for burning-rate law
E_a	=	activation energy of surface reaction
n	=	exponent for burning-rate law
P	=	pressure
Rr_b	=	ratio of transient (dynamic) burning rate to steady-state burning rate
R_u	=	universal gas constant
r_b	=	regression rate
T	=	temperature
$T_{s,0}$	=	burning surface temperature for steady-state condition
t	=	time
x	=	distance measured from the burning surface of propellant to the gas-phase site
α	=	thermal diffusivity of propellant
γ	=	Novozhilov's stability parameter defined by Eq. (12)
Δp_{ndm}	=	nondimensional pressure difference set equal to 2.5
η	=	dimensionless spatial variable
κ	=	Novozhilov's stability parameter defined by Eq. (11)
λ_c	=	thermal conductivity of condensed phase
σ_p	=	temperature sensitivity of propellant defined by Eq. (8)
τ	=	nondimensional time or characteristic time
τ_{Ramp}	=	nondimensional time until which a constant ramping takes place
$\phi_{c,s}$	=	temperature gradient immediately beneath the burning surface of propellant

Subscripts

c	=	condensed-phase, characteristic quantity
f	=	final
g	=	gas phase
i	=	initial
max	=	maximum
ref	=	reference value
s	=	surface
0	=	steady-state value

I. Introduction

THE instantaneous burning rate under rapidly changing pressure condition in rockets and gun systems could be significantly different from the steady-state burning rate measured in a strand burner. Under transient conditions with large-amplitude pressure variations, the instantaneous regression rate cannot be determined solely by the instantaneous pressure level, largely because of the delayed time response of the thermal profile in the solid propellant. Because of the importance of the transient burning process (also called dynamic burning process) in various propulsion systems, this topic has been studied both theoretically and experimentally by various researchers, as described in two book chapters.[1,2] A review of the physical phenomena and various pioneering work was given by Kuo and Coates.[3] Essentially, the transient burning phenomenon is caused by the finite time lags associated with adjustment of 1) temperature profiles in the unreacted solid-phase and surface reaction zone and 2) the energy release rate and flame structure in the gas-phase zone.

It has been observed experimentally that the transient burning effect depends on a large number of parameters, including maximum pressurization rate, the entire history of the pressure-time curve, temperature sensitivity, pressure exponent of the propellant, exothermic heat release at the surface reaction zone, activation energy of the propellant, initial temperature of the propellant, and its thermal properties, etc.[3]

Physically, the transient burning effect is introduced during rapid pressure changes by the finite time interval required for temperature profiles inside the condensed phase, and possibly the reaction zone, to follow transient pressure variations. The faster the pressure changes, the longer the time (relative to the characteristic time of the pressure change) required for temperature profiles to adjust themselves to the new condition. Until temperature profiles in the solid phase and the surface reaction zones are adjusted to the shape

Presented as Paper 2003-5270 at the AIAA/ASME/SAE/ASEE 39th Joint Propulsion Conference and Exhibit, Huntsville, AL, 20–23 July 2003; received 29 August 2003; revision received 11 April 2005; accepted for publication 10 May 2005.

*Distinguished Professor of Mechanical Engineering and Director of High Pressure Combustion Laboratory, Department of Mechanical and Nuclear Engineering. Fellow AIAA.

†Research Staff, Department of Mechanical and Nuclear Engineering.

corresponding to the steady-state burning condition at the new pressure, there is an out-of-phase blowing effect of the chemically reacting gases leaving the burning surface.

Study of dynamic burning characteristics of propellants is complicated by the difficulty of obtaining highly transient data related to the phenomenon occurring in the gaseous flame. Several theoretical models describing the transient burning phenomena of solid propellants were developed by considering the structure of gas-phase flame behavior.[4–7] However, all gas-phase flame structure models depend strongly upon the detailed heat-release profile in the thin flame zone of solid propellants. There is a significant amount of uncertainty in detailed measurements of solid-propellant flames in order to deduce the energy release rate distribution, especially in the early years from the 1960s through the 1970s. Even now, with significant advancements in laser-based diagnostic instrumentation, detailed measurement of energy release rate in solid-propellant flames still has numerous limitations.[8] To bypass this kind of difficulty in describing the flame zone structure, Zel'dovich[9] suggested a way in which the heat feedback to the solid propellant immediately beneath the burning surface could be found using 1) the steady-state experimental data, 2) the Arrhenius form of the propellant pyrolysis law, and 3) the relationship between the energy flux at burning surface and the energy gained from the initial temperature of the propellant to the surface temperature.

Thus, following Zel'dovich's procedure, to study the dynamic burning rate of a propellant, it is possible to bypass all detailed flame structure analysis by solving only the one-dimensional transient energy equation in the condensed phase, if the quasi-steady flame assumption is satisfied (i.e., $\tau_g \ll \tau_p$ and $\tau_c \sim \tau_p$). This implies that the gas-phase relaxation time τ_g is much shorter than the characteristic time associated with pressure variation τ_p, while the condensed-phase relaxation time τ_c can be in the same order magnitude as τ_p. Assuming that there is no subsurface heat generation, the energy equation can be written as

$$\frac{\partial T}{\partial t} + r_b \frac{\partial T}{\partial x} - \alpha_c \frac{\partial^2 T}{\partial x^2} = 0 \qquad [-\infty \le x \le 0] \tag{1}$$

The initial condition is

$$T(x, 0) = T_i + (T_{s,0} - T_i) \exp(r_b x/\alpha_c) \tag{2}$$

The cold-end boundary condition is

$$T(-\infty, t) = T_i \tag{3}$$

The boundary condition just beneath the burning propellant surface is

$$\frac{\partial T}{\partial x}(0^-, t) = \phi_{c,s}[r_b(t), P(t)] \tag{4}$$

Zel'dovich map[1] provides the temperature gradient function from the definition of $\phi_{c,s}(r_b, P)$, that is,

$$\phi_{c,s}(r_b, P) \equiv \left.\frac{\partial T}{\partial x}\right|_{\text{Burning Surface}} = \frac{r_b(T_s - T_i)}{\alpha_c} \tag{5}$$

JA2 is a modified double-base gun propellant used in various propulsion systems. It consists of 59.50% nitrocellulose (with 13.14% N), 14.90% nitroglycerin, 24.80% diethylene glycol dinitrite, 0.70% N′-methyl-N-N-diphenylurea (Akardite II), 0.05% magnesium oxide, and 0.05% graphite by weight. Some steady-state burning data and transient burning behavior of JA2 were reported by Kuo and coworkers[10,11] using various methods, as well as by Eisenreich et al.[12] and Miller.[13] Some burning-rate data were obtained from closed-bomb testing by the U.S. Army. However, it is difficult to determine the burning surface temperature and the temperature profiles using the closed-bomb method. Therefore, optical strand burner was adopted not only to study the steady-state burning-rate behavior but also the thermal profile of the JA2 propellant under various operating conditions.

II. Experimental Approach

A high-pressure optical strand burner was utilized to conduct experiments on JA2 propellant strands. The system has a windowed stainless-steel chamber (with viewing area of 9.5×3.2 cm), an electric heater, and a cryogenic chiller to control the sample initial temperature at a desirable level by the heated or chilled purge gas. S-type fine-wire thermocouples made of pure platinum and 10% rhodium/platinum bare wires were embedded in the sample to measure the temperature profile and propellant initial temperature controlled by the purge gas temperature. The chamber can withstand a maximum operating pressure of around 68 MPa. A purge gas pressurization and exhaust system is utilized with the optical chamber, in order to provide the desired pressure environment. A Setra Model 206 pressure transducer was used to monitor the chamber pressure, which is controlled at a fixed level during the test. The chamber has several diagnostic ports, through which break wire and thermocouple signals are obtained from the tested propellant strand. The signals are fed to a multichannel data-acquisition system for storage and analysis.

In strand burner tests, JA2 propellant samples of the following specifications were used. The overall sample length was about 5.7 cm, and the diameter was 0.635 cm. It consisted of two pieces. On the bottom end of the longer piece, an inverted conical cup space was accurately machined, whereas on the top end of the shorter piece a truncated cone with a flat top was machined to match exactly with the cup space. At the matched interface, a fine-wire S-type thermocouple with an average thickness on the order of 2–5 μm was embedded in the sample at a distance about 3.5 cm from the top of the sample. The thermocouple was carefully installed on the platform of the truncated cone surface under a microscope. Then the cup and cone sample elements were joined together with a specially constructed sample holder for connecting them under a selected force loading. A small amount of epoxy was used on the lateral surface around the connecting station, which is offset from the thermocouple bead station. After the two sample elements were rigidly connected, a small piece of igniter propellant with a Nichrome alloy wire for energy supply was affixed to the top of the sample. The propellant sample was then coated on the lateral surface with a clear fingernail polish to prevent the flame from spreading along the lateral surface, thereby the regression takes place in a one-dimensional manner along the axis of the sample. Two break wires (0.12-mm-diam fuse wire) were installed at 2 cm apart from each other to obtain propellant burning rate in addition to visual records; these wires were mounted above the thermocouple junction station.

III. Experimental Results and Discussion

A. Regression Rate and Temperature Sensitivity

The regression-rate data were reduced, compiled, and correlated. Several correlations were established using the data for broad ranges of pressure and initial temperatures. All of the burn-rate data were correlated to the following expression:

$$r_b = a P^n \exp[\sigma_p (T_i - T_{i,\text{ref}})] \tag{6}$$

where $T_{i,\text{ref}} = 298$ K and σ_p represents the temperature sensitivity, which in general is a function of pressure. Comparison of the correlated burning-rate expression of JA2 propellant with the measured burning rates, including some high-pressure data obtained earlier at the Pennsylvania State University and U.S. Army, is shown in Fig. 1.

The temperature sensitivity σ_p shown in Eq. (7) was considered as a function of pressure according to the following expression:

$$\sigma_p = \sigma_{p,c} + b/(c_1 + c_2 P) \tag{7}$$

As usual, the definition of temperature sensitivity σ_p is given by Eq. (8):

$$\sigma_p \equiv \left.\frac{\partial \ell n\, r_b}{\partial T_i}\right|_P \tag{8}$$

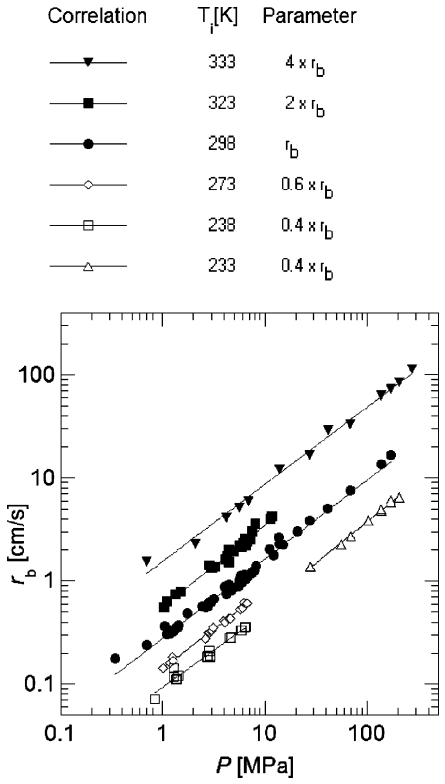

Fig. 1 Comparison of correlated burning-rate expression of JA2 propellant with the measured burning-rate data.

Note that this definition does not have any conflict with the consideration for σ_p to be a function of pressure. One can verify this point by differentiating the natural log of Eq. (6). The parameter values obtained from the burning-rate curve-fitting procedure are

$$a = 0.2478\ (\text{cm/s})\ (\text{MPa})^{-n}, \qquad n = 0.8222$$

$$\sigma_{p,c} = 0.00240\ \text{K}^{-1}, \qquad b = 0.0537\ \text{K}^{-1}$$

$$c_1 = 17.0425, \qquad c_2 = 2.2108\ \text{MPa}^{-1}$$

The initial temperature of the samples was between 233 and 333 K. It is obvious that the overall burning-rate correlation is valid for a broad range of temperatures as shown in Fig. 1. All data points, plotted in terms of burning rates multiplied by different factors for the purpose of separating data obtained from different initial temperatures, lie on corresponding correlation curves. This indicates close agreement between the correlation and experimental data. The functional form of the correlation is represented by Eq. (6) with the pressure-dependent σ_p from Eq. (7) and the constants just given.

Figure 2 shows σ_p of JA2 propellant as a function of pressure. It is apparent from the plot that for the high-pressure range σ_p does not vary significantly and approaches asymptotically to $\sigma_{p,c}$. In the low-pressure range ($p < 20$ MPa), however, temperature sensitivity falls sharply with increase of pressure.

B. Propellant Surface-Temperature Determination

Figure 3 shows a typical experimentally measured temperature profile in JA2 propellant on two different scales; a T-t plot and a $\ell_n(T\text{-}T_i)$ vs time plot. From this experimentally measured temperature profile, it was observed that the natural log plot showed a linear behavior in the region beneath the burning surface as indicated by the overlapped region of the tangent line to the curve. In the low-temperature range close to T_i, the natural log curve showed some variance, which is normal and caused by the noise for temperature variations within 1 or 2 degrees K. The departure point from the tangent line after the overlapped region is selected as the time when the thermocouple bead reached the burning surface of the propellant.

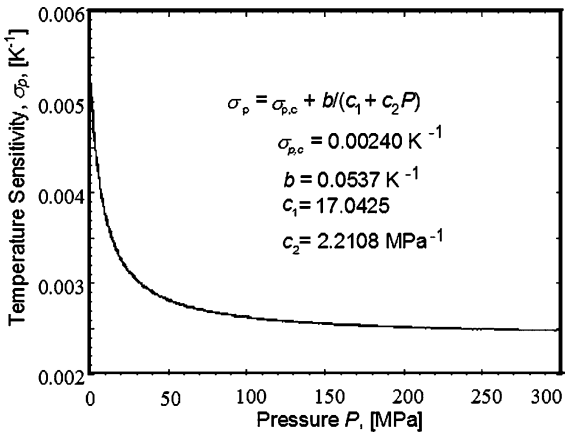

Fig. 2 Temperature sensitivity of JA2 propellant as a monotonically decreasing function of pressure.

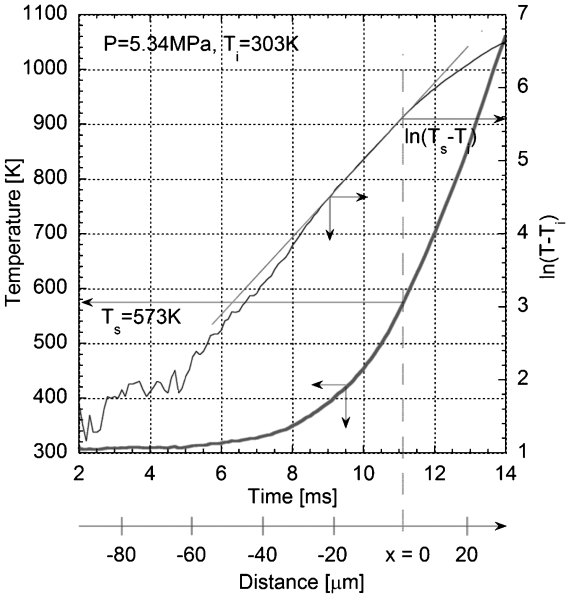

Fig. 3 Measured temperature profile and the corresponding plot of $\ell_n(T\text{-}T_i)$ vs t for burning JA2 propellant surface-temperature determination ($P = 5.34$ MPa, $T_i = 303$ K).

The corresponding temperature is therefore selected as the surface temperature T_s.

As shown in Fig. 3, at the propellant burning surface there is a noticeable change of slope from the tangent line to the $\ell_n(T\text{-}T_i)$ curve. On the coordinate perpendicular to the surface, the burning surface is considered to be at $x = 0$ position. The negative x values correspond to the points in the subsurface region of the solid propellant, while the positive values of x correspond to the burnt gas region. The subsurface heat generation does not seem to be significant at all in JA2 propellant. This can be supported by the fact that if any noticeable heat generation were occurring then there should be a bump showing a rise in temperature near the burning surface in $\ell_n(T\text{-}T_i)$ curve of the temperature profile, instead of a close match with the tangent line for more than 30-μm distance below the burning propellant surface.

Figure 4 shows a three-dimensional plot of surface temperature of JA2 as a function of initial temperature T_i and pressure P with pressures less than 9 MPa. For the range of pressure for which surface temperatures were available from experiments, a pressure and initial temperature-dependent relationship shown by Eq. (9) was chosen based upon the curve-fitting results.

$$T_s = (a_0 + a_1 T_i) + (b_0 + b_1 T_i) P \tag{9}$$

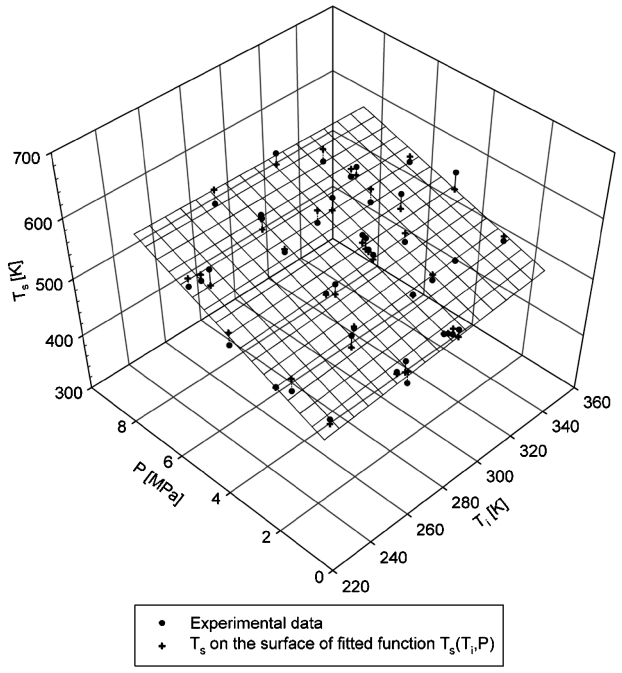

Fig. 4 Correlation of JA2 propellant burning surface temperature vs initial temperature and pressure (for $P < 9$ MPa).

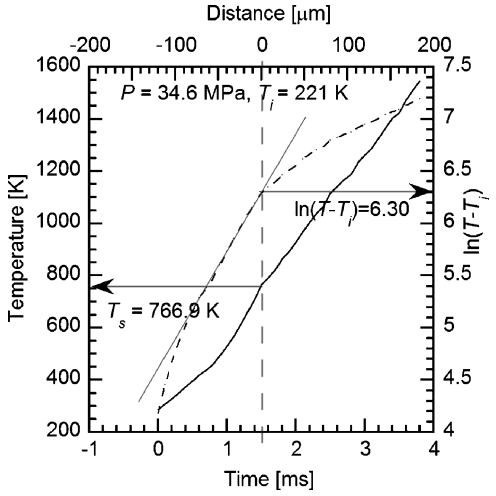

Fig. 5 Microthermocouple trace for JA2 propellant burning at 34.6 MPa (5000 psig) with initial temperature of 221 K.

which is the equation of a plane. The parameters obtained for Eq. (9) are $a_0 = 382.862$ K, $a_1 = 0.2883$, $b_0 = 28.2059$ K MPa^{-1}, and $b_1 = -0.0406$ MPa^{-1}. The departure of the measured surface temperature (dot data points) from that predicted by the correlation (cross points on the correlation plane) is shown in Fig. 4 by the vertical distance between the dot and cross points. The average error is about ±25 K.

A linear fit is not valid for high-pressure data much greater than 9 MPa. A microthermocouple trace for JA2 propellant burning at 34.6 MPa (5000 psig) with initial temperature of 221 K is shown in Fig. 5. The surface temperature is near 766.9 K. The burning surface temperature generally increases with pressure; however, the value of dT_s/dP decreases very significantly with the increase of pressure for the low-pressure range ($P < 20$ MPa). Beyond 20 MPa, the slope decreases continuously as pressure increases. For high-pressure range ($P > 30$ MPa), the slope reaches nearly a constant value.[11] A relation that predicted the trend of the surface-temperature variation with pressures for double-base propellant was also suggested by Zenin.[14]

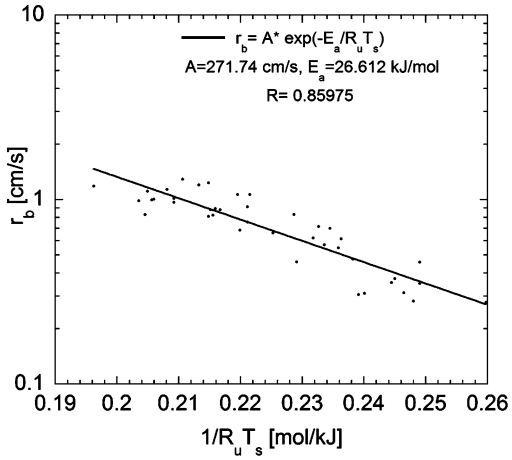

Fig. 6 Burning-rate vs $1/R_u T_s$ for obtaining the activation energy of JA2 propellant at low pressures ($P < 9$ MPa).

The activation energy for a low-pressure regime ($P < 9$ MPa) of the JA2 propellant was derived using the experimentally obtained regression rate and the surface temperature. The burning rate was plotted against $1/R_u T_s$ in Fig. 6 on a semilog plot and fitted with a straight line. The activation energy E_a was obtained from the slope of the line. For this low-pressure regime, the value of E_a was found to be 26.61 kJ/mol with preexponential Arrhenius coefficient A of 271.74 cm/s. Essentially, using this set of values one can obtain the propellant burning rate from surface temperature in degrees Kelvin with the following Arrhenius equation for this low-pressure regime. In Eq. (10), the regression rate is given in centimeters/second and the surface temperature in degrees Kelvin:

$$r_b = A \cdot \exp[-E_a/R_u T_s] \tag{10}$$

In this work, a correlation with BT^β to replace A in Eq. (10) was attempted initially. However, the best correlation was obtained with A as a constant.

The activation energy of the JA2 propellant is a function of pressure. In a different pressure regime, the value was found to be around 47 kJ/mole, based upon the data of Kopicz et al.[10] For a higher-pressure regime, Lengelle et al.[15] reported that the E_a values for double-base propellants lie around 71 to 84 kJ/mole. The change of activation energy with respect to pressure can be regarded by the influence of pressure on chemical reaction mechanism. For example, certain three-body reactions can become more important at high-pressure conditions. In the current study, we are particularly interested in the relatively low-pressure regime because σ_p has very steep variations at low pressures ($P < 20$ MPa).

C. Novozhilov Stability Parameters

Novozhilov stability parameters κ and γ, defined by Eqs. (11) and (12), were determined from the experimental data. Their mathematical definitions are

$$\kappa \equiv (T_s - T_i)\sigma_p \tag{11}$$

$$\gamma \equiv \left(\frac{\partial T_s}{\partial T_i}\right)_p \tag{12}$$

Using the correlated results of T_s with P and T_i given in Eq. (9), γ is deduced as

$$\gamma = a_1 + a_2 P \tag{13}$$

According to Novozhilov Stability criteria,[2] a solid propellant is stable 1) if either $\kappa < 1$ 2) or if $\kappa > 1$, then $\gamma > \gamma^*$, where $\gamma^* \equiv (\kappa - 1)^2/(\kappa + 1)$. From the plot of κ vs T_i and P (Fig. 7), it is observed that $\kappa < 1$ for some region of the two operating variables $[P, T_i]$, while $\kappa > 1$ for the rest of the region. Therefore, one has to

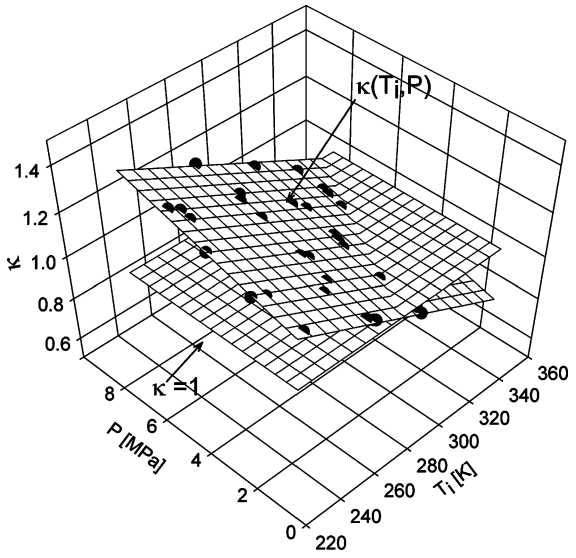

Fig. 7 Plot of JA2 stability parameter κ vs initial temperature and pressure.

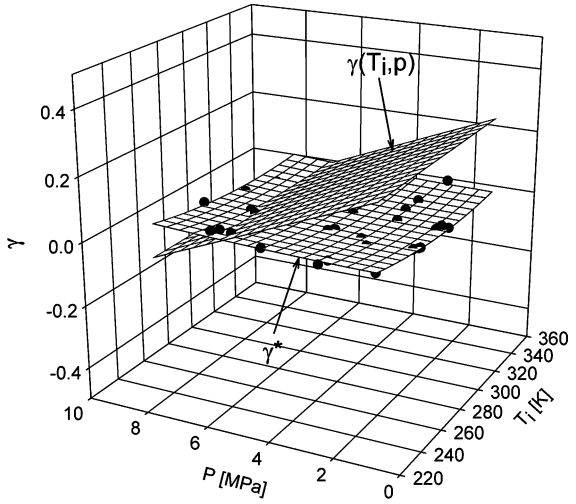

Fig. 8 Comparison of JA2 stability parameter γ surface with the γ^* surface.

compare γ surface with γ^* surface as well. From the plot of γ and γ^* surfaces vs T_i and P shown in Fig. 8, it is found that the γ surface is above the γ^* surface for the ranges of pressures less than 7 MPa at various initial temperatures. The γ surface is a plane because of the linear correlation of T_s. If a different function were selected, the surface could have been a little different. Nevertheless, it cannot be concluded that JA2 propellant can burn in a stable manner for the operating range indicated by just considering the Novozhilov stability parameters. We need to consider the Zel'dovich map for more detailed analysis of transient burning behavior.

D. Zel'dovich Map Construction

The Zel'dovich map of JA2 propellant was constructed using the experimentally obtained parameters and relations. Figure 9 shows the Zel'dovich map of JA2 propellant, which essentially shows the temperature gradient immediately beneath the burning surface as a function of regression rate for different P and T_i. The procedure of construction of the Zel'dovich map has been described by Kuo et al.[1] Under very rare situation, the Zel'dovich map is available for a given solid propellant, caused largely by the extensive data requirement for broad ranges of test conditions.

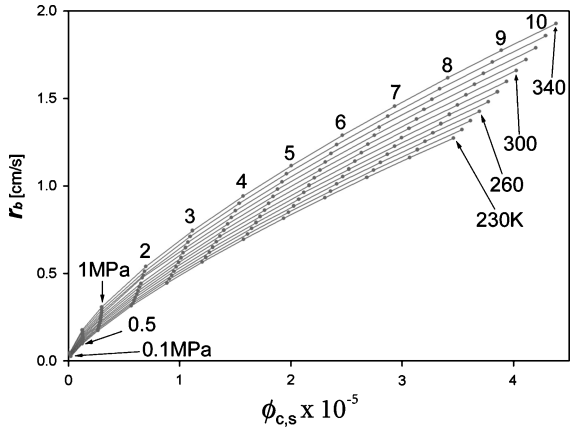

Fig. 9 Zel'dovich map of JA2 propellant showing regression rate vs temperature gradient at burning surface for different pressures and initial temperatures.

IV. Dynamic Burning Simulation Results and Discussion

A dynamic burning simulation was performed using the Zel'dovich approach. Essentially, the Zel'dovich map was used as one of the boundary conditions for the transient energy equation [Eq. (1)]. It was assumed that there is no subsurface heat release in JA2 propellant, as has been supported by the temperature profiles recorded. If there is any noticeable subsurface heat release, the Zel'dovich approach cannot be applied.

Invariant imbedding scheme was used in the solution of the nonlinear equation with rapidly rising external pressure imposed on the burning environment to find out various quantities of interest. Kooker and Nelson[16] showed that this scheme works best for the type of equation in consideration. They have described the invariant imbedding scheme in detail. Theoretical treatment of this method was also presented by Meyer.[17] This numerical scheme is unconditionally stable.[16] It is first-order accurate in time and second-order accurate in space, that is, $\mathcal{O}(\Delta\tau, \Delta\eta^2_{\max})$. The time and distance variables (t and x) were made dimensionless, and the calculations were performed in nondimensional form. Later on the quantities were reverted to dimensional form. Because the problem involves a thermal profile, which might have very steep gradients near the burning surface, the spatial mesh was closely spaced in this region (i.e., $\Delta\eta \ll 1$). A 231-grid point system (21 points in the region $-0.01 \le \eta \le 0$; 30 points in the region $-0.10 \le \eta \le -0.01$; 50 points in the region $-2.00 \le \eta \le -0.10$; 130 points in the region $-15.00 \le \eta \le -2.00$) was selected for the calculation. The different quantities used in the calculations are described next.

$$r_{b0} = 0.2476 \text{ cm/s}, \qquad T_{s,0} = 389.3 \text{ K}, \qquad T_i = 298.0 \text{ K}$$

$$t_c = 21.53 \text{ ms}, \qquad \tau \equiv t/t_c = t \cdot \left(r_{b0}^2/\alpha_c\right)$$

$$\tau_i = 0.0, \qquad \tau_f = 3.0, \qquad \Delta\tau = 0.01$$

$$x_c = 53.31\ \mu\text{m}, \qquad \eta \equiv x/x_c = x \cdot (r_{b0}/\alpha_c), \qquad \eta_0 = -15.00$$

$$\alpha_c = 1.32 \times 10^{-7}\ \text{m}^2/\text{s}, \qquad P_0 = 1.00 \text{ MPa}, \qquad \Delta p_{\text{ndm}} = 2.5$$

In the following sections, the results of the simulation are presented. The purpose of this study was to compute the burning rate response to a rapidly increasing pressure excursion. For simulating abrupt pressure increase, ramp-type profiles as described by Eqs. (14a) and (14b) were selected with different initial pressurization rates. The maximum pressure was chosen to be the same for all of the cases, but the value of τ_{Ramp} is different for different cases.

The pressure profile is a ramp starting at P_0 and rising at a certain pressurization rate $\mathrm{d}P/\mathrm{d}t$ and then remaining at constant pressure

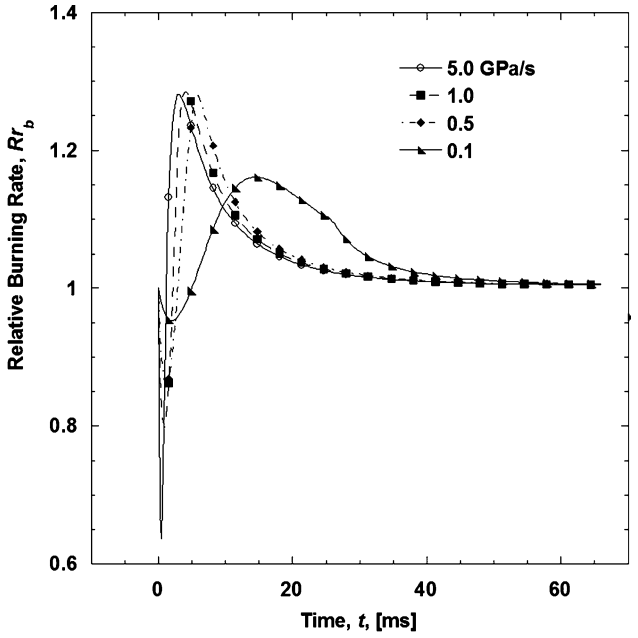

Fig. 10 Time variations of the ratio of dynamic burning rate to steady-state burning rate for four different pressurization rates.

of $P_0[1.0 + \Delta p_{\text{ndm}}]$ after $\tau = \tau_{\text{Ramp}}$ defined by

$$P(t) = P_0[1.0 + \Delta p_{\text{ndm}}(\tau/\tau_{\text{Ramp}})] \qquad \text{for} \qquad 0 \le \tau \le \tau_{\text{Ramp}} \tag{14a}$$

$$P(t) = P_0[1.0 + \Delta p_{\text{ndm}}] \qquad \text{for} \qquad \tau > \tau_{\text{Ramp}} \tag{14b}$$

Four different pressure profiles were chosen with initial pressurization rates of 0.1, 0.5, 1.0, and 5.0 GPa/s.

Figure 10 shows the time variation of the ratio of dynamic burning rate to steady-state burning rate Rr_b, calculated using the pressure profile and steady-state burning-rate law [Eq. (6)]. At first, the ratio Rr_b falls below one, indicating that the thermal profile, which controls the burning rate, does not respond instantaneously to the increasing pressure. One can observe a slight increase in the burning rate near the initial part of the profile. The maximum overshoot value of Rr_b is around 1.28, signifying a relatively weak dynamic burning effect of JA2 propellant. After the initial transient period Rr_b reaches the steady-state value of unity for all cases studied.

The calculated subsurface temperature profiles in JA2 propellant for different times in the dynamic burning event under different pressurization rates indicated that the surface temperature has to first catch up with the pressure increase resulting in negative dynamic burning effect (with $Rr_b < 1$) during the initial period. Later on, the thermal profile in the condensed phase exhibited the preheat effect caused by the thermal energy storage in the propellant, while burning under lower pressure conditions. Essentially, the temperature profiles cross over during the development process in the transient period of pressure excursion. The temperature gradient immediately beneath the burning surface is higher during the times when the burning rate is higher than the steady-state burning rate.

To determine the degree of transient burning-rate response of JA2 propellant, a series of experimental tests was conducted using an interrupted burner with X-ray translucent windows that permit observation of the propellant sample during combustion. This test rig is also equipped with rupture diaphragms of different thicknesses. The instantaneous burning rates of JA2 propellant rods were determined using X-ray radiography images and a modified interior ballistic burning-rate analysis code[18] for data reduction. Also, immediately following the rupture of the diaphragm, the chamber pressure decreased rapidly, thereby extinguishing the propellant samples. During the rapid depressurization, the propellant samples are retained within the test chamber and recovered later for postfiring examination. The experimental setup of these tests is similar to that described

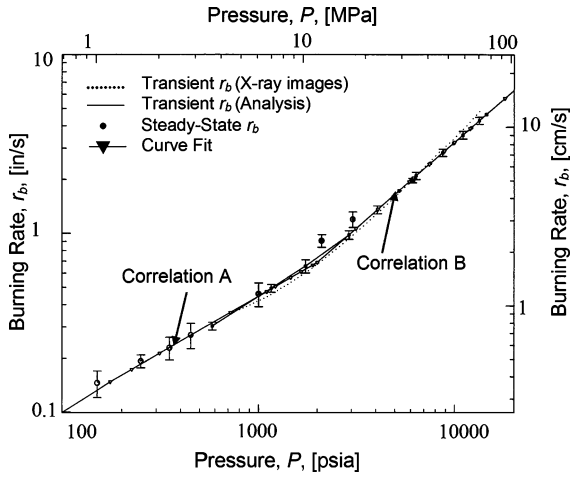

Fig. 11 Comparison of transient (dynamic) burning rates measured from an interrupted windowed burner to steady-state burning rates of JA2 propellant at various pressure levels.

in the work of Watson et al.[11] To achieve different chamber pressurization rates, different propellant loading fractions were used. The maximum chamber pressurization rate attained was 11,000 MPa/s. The transient burning rates of these tests were compared with the steady-state burning rates of JA2 propellant as well as the room-temperature burning-rate correlations in Fig. 11. It is quite obvious that the differences are very small. For the relatively low-pressure regime (below 13.8 MPa), the r_b correlation at room temperature can be represented by correlation A:

$$r_b \text{ (cm/s)} = 1.127[P(\text{MPa})/6.894]^{0.63} \qquad \text{for} \qquad 0.70 < P < 13.8 \text{ MPa} \tag{15a}$$

For the high-pressure regime (above 13.8 MPa), the r_b correlation at room temperature can be represented by correlation B:

$$r_b \text{ (cm/s)} = 5.822[P(\text{MPa})/48.26]^{0.97} \qquad \text{for} \qquad 13.8 < P < 96.5 \text{ MPa} \tag{15b}$$

This experimental verification further supports the theoretical finding that transient burning effect of JA2 propellants is quite insignificant.

V. Conclusions

1) A generalized burning-rate correlation of the JA2 propellant as a function of pressure and initial temperature was developed to cover a broad range of pressures up to 300 MPa and initial temperature from -40 to 80°C. The correlated burning rate compares very closely with measured data.

2) Temperature sensitivity of JA2 propellant was found to decrease drastically as the pressure is increased to about 30 MPa; it then reaches an asymptotic value of 0.0024 K^{-1} at very high pressures.

3) Surface-temperature data for JA2 were determined from the fine-wire thermocouple traces measured from strand burning tests. The surface temperature was correlated with pressure ($P < 9$ MPa) and initial temperature ($-40 < T_i < 80$°C) as a linear function of pressure with coefficients dependent on the initial temperature. This function was very helpful for the development of the Arrhenius pyrolysis law, which was utilized in the construction of the Zel'dovich map.

4) The Zel'dovich map of JA2 propellant was constructed and used in the study of the dynamic burning characteristics. The results indicated that JA2 propellant does not have significant dynamic burning effects in the range of test variables considered. The main reason for the weak dynamic burning effect seems to be the low value of the temperature sensitivity σ_p and its rapid decay as the pressure increases in the low-pressure region ($P < 20$ MPa).

5) Experimental results obtained from a series of test firings using an interrupted burner with X-ray translucent windows also verify theoretical finding that transient burning effect of JA2 propellants is quite insignificant, even the chamber pressurization rate was up to 11,000 MPa/s.

Acknowledgments

We would like to thank the support of Army Research Office for the project under Grant DAAD19-01-1-0573 funded by David M. Mann. His sponsorship is greatly appreciated. A portion of this work was also funded by the SOREQ Nuclear Research Center, Yavne, Israel, through the contract (Contract 379/5457-99) with Shlomo Wald. The authors would like to thank him for his support. Thanks to Surajit Kumar of the Pennsylvania State University for his assistance in the early portion of this work.

References

[1]Kuo, K. K., Gore, J. P., and Summerfield, M., "Transient Burning of Solid Propellants," *Fundamentals of Solid-Propellant Combustion*, edited by K. K. Kuo and M. Summerfield, Progress in Astronautics and Aeronautics, Vol. 90, AIAA, New York, 1984, Chap. 15, pp. 599–660.

[2]Novozhilov, B. V., "Theory of Nonsteady Burning and Combustion Stability of Solid Propellants by the Zel'dovich-Novozhilov Method," *Nonsteady Burning and Combustion Stability of Solid Propellants*, edited by L. De Luca, E. W. Price, and M. Summerfield, Progress in Astronautics and Aeronautics, Vol. 143, AIAA, Washington, DC, 1992, Chap. 15, pp. 601–641.

[3]Kuo, K. K., and Coates, G. R., "Review of Dynamic Burning of Solid Propellants in Gun and Rocket Propulsion Systems," *16th Symposium (International) on Combustion*, The Combustion Institute, Pittsburgh, PA, 1976, pp. 1117–1192.

[4]Krier, H., T'ien, J. S., Sirignano, W. A., and Summerfield, M., "Nonsteady Burning Phenomena of Solid Propellants: Theory and Experiments," *AIAA Journal*, Vol. 6, No. 2, 1968, pp. 278–285.

[5]Kooker, D. E., and Zinn, B. T., "Numerical Investigation of Non-Linear Axial Instabilities in Solid Rocket Motors," U.S. Army, BRL, Contract Rept. 141, Aberdeen, MD, March 1974.

[6]Levine, J. N., and Culick, F. E. C., "Nonlinear Analysis of Solid Rocket Combustion Instability," U.S. Air Force, AFRPL TR-74-45, Edwards, CA, Oct. 1974.

[7]T'ien, J. S., "Oscillatory Burning of Solid Propellants Including Gas Phase Time Lag," *Combustion Science and Technology*, Vol. 5, No. 47, 1972, pp. 47–54.

[8]Kuo, K. K., and Parr, T. P. (eds.), *Non-Intrusive Combustion Diagnostics*, Begell House, New York, 1994, p. 754.

[9]Zel'dovich, Ya. B., "On the Theory of Propellant Combustion," *Zhurnal Eksperimental'noi o Theoretischeskoi Fiziki*, Vol. 12, No. 11–12, 1942, pp. 498–524.

[10]Kopicz, C., Watson, T. J., Kuo, K. K., and Thynell, S. T., "Combustion Behavior and Thermochemical Properties of JA2 Propellant," *Challenges in Propellants and Combustion 100 Years After Nobel*, edited by K. K. Kuo, T. B. Brill, R. A. Pesce-Rodriguez, A. R. Mitchell, J. Covino, S. K. Chan, A. Peretz, N.-E. Gunners, S. T. Thynell, and S. H. Chan, Begell House, New York, 1997, pp. 559–573.

[11]Watson, T. J., Kuo, K. K., and Thynell, S. T., "The Assessment of Dynamic Burning Behavior for JA2 Propellant Rods," *31st JANNAF Combustion Sub-Committee Meeting*, CPIA Publ. 620, Vol. 2, 1994, pp. 247–257.

[12]Eisenreich, N., Weiser, V., Eckl, W., Fischer, T., Kelzenberg, S., and Langer, G., "Combustion Phenomenon of The Gun Propellant JA2," *Combustion of Energetic Materials*, edited by K. K. Kuo and L. T. De Luca, Begell House, New York, 2001, pp. 251–262.

[13]Miller, M. S., "Thermophysical Properties of Six Solid Gun Propellants," Army Research Lab., Rept. A098223, Aberdeen Proving Ground, MD, March 1997.

[14]Zenin, A. A., "Thermophysics of Stable Combustion Waves of Solid Propellants," *Nonsteady Burning and Combustion Stability of Solid Propellants*, edited by L. De Luca, E. W. Price, and M. Summerfield, Progress in Astronautics and Aeronautics, Vol. 143, AIAA, Washington, DC, 1992, Chap. 6, pp. 197–231.

[15]Lengelle, G., Bizot, A., Daterque, J., and Trubert, J. F., "Steady-State Burning of Homogeneous Propellants," *Fundamentals of Solid Propellant Combustion*, edited by K. K. Kuo and M. Summerfield, Progress in Astronautics and Aeronautics, Vol. 90, AIAA, New York, 1984, Chap. 7, pp. 361–407.

[16]Kooker, D. E., and Nelson, C. W., "Numerical Solution of Solid Propellant Transient Combustion," *Journal of Heat Transfer*, Vol. 101, 1979, pp. 359–364.

[17]Meyer, G. H., *Initial Value Methods for Boundary Value Problems (Theory and Application of Invariant Imbedding)*, edited by R. Bellman, Mathematics in Science and Engineering Series, Academic Press, New York, 1973, p. 270.

[18]Oberle, W. F., and Kooker, D. E., "BRLCB: A Closed-Chamber Data Analysis Program Part I—Theory and User's Manual," U.S. Army, ARL-TR-36, Aberdeen, MD, Jan. 1993.